



# Ant Lion Optimized Hybrid-Fuzzy-PID Controller for Frequency-Voltage Regulation in Hybrid Power System

Sanni Kumar<sup>1</sup> and Amit Kumar<sup>1</sup>

<sup>1</sup>Department of Electrical Engineering, National Institute of Technology, Kurukshetra, Haryana, India

Received 1 May. 2022, Revised 1 May. 2023, Accepted 14 May. 2023, Published 30 May. 2023

**Abstract:** This paper proposes an optimal Hybrid Fuzzy PID plus PID controller for frequency and voltage regulation of the Hybrid power system (HPS) under numerous conditions. The controller's parameters are optimally tuned using Ant Lion Optimization (ALO). The suggested optimization outperforms recently published algorithms as the whale optimization algorithm (WOA), grey wolf optimization (GWO), and salp swarm algorithm (SSA). Comparing the results of the suggested controller to those of PI, PID, and Fuzzy PID (FuPID) for the same system with parameters tuned using Ant Lion Optimization (ALO) demonstrates the superiority of the suggested controller. Further, with a proposed controller optimized using ALO, the value of the ITAE, one of the performance measures, is reduced by 89.75%, 89.95%, and 85.52% compared with optimization of the suggested controller using GWO, SSA and WOA, respectively. The robustness of ALO optimised proposed controller is tested with a Parametric variation of  $\pm 20\%$ . The proposed optimised hybrid controller displays the best performance of all the controllers used here. MATLAB\Simulink was used to perform simulations and modelling.

**Keywords:** Ant Lion Optimization, Hybrid Power System, Frequency regulation, Voltage regulation, Fuzzy Logic Control.

## 1. INTRODUCTION

Lack of access to energy is one of the most severe issues in rural communities. It is reasonably due to their inaccessibility, making the conventional grid expansion economically unfeasible [1]. The rise in demand for electrical energy, the limitation of conventional fuels and this environmental issue leads to faster development of renewable energy sources (RES) at the nation and individual level [2]. Because the unpredicted nature of RESs impacts the optimal power flow, power quality, voltage and frequency control, etc. The fundamental control challenge for practising engineers is the small perturbation of nominal voltage and frequency level in electric power systems. Any deterioration in these two characteristics will impact the operational life span of the power system's related equipment [3]. The controller for the power system's automatic generation and control (AGC) should have outstanding disturbance rejection capabilities. As a result, utilizing an imperialist competitive algorithm for multi-area power systems, Ref [4] proposed a fuzzy assisted integer-order PID with filter-fractional order integral controller. Ref [5] used genetic algorithms (GA) optimization technique to develop and implement both centralised and decentralised PID-structured AGC controllers. resulting in optimal controller parameters. A GWO-based FuPID controller was presented for the LFC of a two-area multi-source system [6]. In the ref [7], SSA was

used to optimally tune the controller consisting of integer order proportional derivative and fractional order tilted integral derivative. Modelling, controllability analysis, as well as the design of aggressive, the interconnected power system by using robust controllers were all addressed in ref [8]. The frequency small perturbation of a distributed power system was performed using a sine adapted enhanced WOA tuned Adaptive Fuzzy PID (AFPID) controller [9],[10]. A cascaded fuzzy FOPI-FOPID controller was presented as an innovative control solution for the AGC problem in ref [11]. Differential Evolution Algorithm based robust Fractional Order  $PI^{\lambda}D$  controller [12], non-fragile PI control (NPI-control) [13], and a new adaptive fractional frequency control method [14] was investigated for LFC methods for an interconnected power system. In the paper [15], The research employed an emotional controller for LFC of HPS in an unregulated environment. This paper [16] used a fast terminal sliding mode controller to consider the LFC of multi-area interconnected systems. Gravitational Search Algorithm (GSA) optimisation-based PID controller was incorporated and applied on the interconnected AGC power system [17]. Ref [18] proposed the hybrid BFPSO tuned PI controller for LFC of interconnected power system. The ref [19] addressed AGC robustness utilising artificial bee colony (ABC) algorithms optimized 2DOFPID. JAYA algorithm-based FuPID controller were suggested for AGC in a multi-area

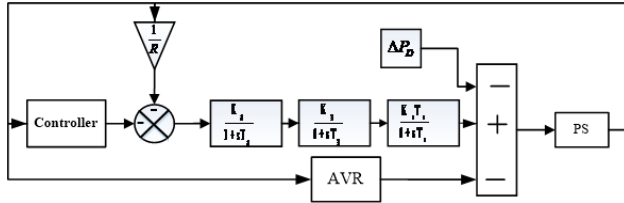


Figure 1. Comparative system for comparison

multi-sources hydrothermal system [20]. The LFC of an HPS comprising a PV system and thermal generators was developed by combining PSO-oriented bacteria foraging optimization algorithm tuning PID controllers [21]. The innovative hybrid controller FuPID + PID for frequency regulation in an HPS was optimized using WOA [22]. The author in the ref [3] used moth flame optimization algorithm for LFC and terminal voltage of power systems simultaneously. The author in the ref [23] shows the comparison between intelligent fuzzy and PSS controlled AVR system. This study implements ALO-based optimal tuning of PI, PID, FuPID, and proposed hybrid-FuPID plus PID controllers for voltage and frequency regulation in an HPS under various operating conditions. A robustness study under large fluctuations in system parameters has also undergone sensitivity analysis. To demonstrate the effectiveness of constructed method under various operating conditions, simulation results are shown.

2. METHODOLOGY

A. Investigated System (System Understudy)

The LFC and AVR models were studied collectively in this study. figure 1 shows the same system which had been already reported by others author [3], The PID controller is optimised using ALO and other evolutionary optimization that had already been already implemented in [3] for comparative analysis to show the ALO algorithm's superiority. The hybrid power system consists of a reheat thermal generator, Wind Generator (WG), Aqua Equalizer (AE), Fuel Cell (FC), Diesel Engine Generator (DEG), and Battery Energy Storage System (BESS) [22], [24]. The proposed method is used for the problem of a physical system like the selection parameter of FuPID for the frequency regulation and voltage deviations. In the presence of wind sources, the system's behavior is very unpredictable. Due to the sporadic nature of wind, the output of wind generator varies on the climate conditions of the specific location; maintaining frequency and voltage deviations are challenging. Figure 2 and Figure 3 demonstrate the transfer function model of above described system.

The ITAE objective function, provided by Equation 1, was used in the optimization, which resulted in a shorter settling time and reduced overshoot.

$$ITAE = \int (|\Delta f| + |\Delta V|) * t * dt \tag{1}$$

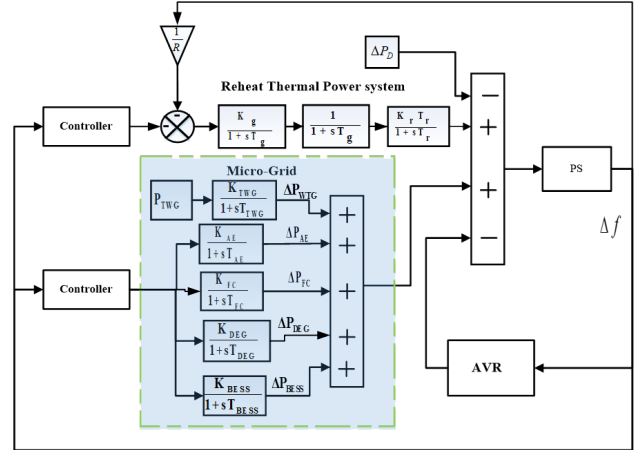


Figure 2. Transfer function model of HPS

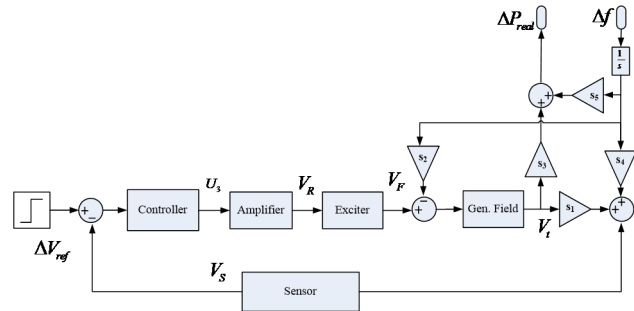


Figure 3. Block diagram of AVR

Wind Turbine Generator (WTG)

Because of the fluctuating wind speed, the WTG output is variable and may be characterized by the standard Equation 2.

$$P_{WT} = \frac{1}{2} \rho A R C_P V_W^3 \tag{2}$$

Though the theory of WTG is well established, a summary is included for the completeness of the paper. A portion of the WTG output is used to manufacture hydrogen, which is then used to generate electricity in the FC. Without accounting for the nonlinearities, The WTG's transfer function is described as follows:

$$G_{WTG} = \frac{\Delta P_{WTG}}{\Delta P_{WT}} = \frac{K_{WTG}}{1 + sT_{WTG}} \tag{3}$$

where  $\Delta P_{WTG}$  and  $\Delta P_{WT}$  are the deviation in WTG output power and available wind power, respectively while  $K_{WTG}$ ,  $T_{WTG}$  are gain and time constant parameters.

Aqua Equalizer (AE)

The transfer function model for AE can be described as follows.

$$G_{AE} = \frac{\Delta P_{AE}}{U_2} = \frac{K_{AE}}{1 + sT_{AE}} \tag{4}$$

where  $\Delta P_{AE}$ , is the AE,  $K_{AE}$  and  $T_{AE}$  are the output power deviation, gain and time constant, respectively.

#### Fuel Cell (FC)

It is an electrochemical device that utilises hydrogen as a fuel to create power. The linearized transfer function can be used to describe the FC.

$$G_{FC} = \frac{\Delta P_{FC}}{U_2} = \frac{K_{FC}}{1 + sT_{FC}} \quad (5)$$

where  $\Delta P_{FC}$  denotes the FC output power deviation,  $U_2$  represents the FC input, also known as controller output, and  $K_{FC}$  is gain and  $T_{FC}$  denotes the time constant parameters, respectively.

#### Diesel Engine Generator (DEG)

DEG is generally in standby mode, however, it will activate if there is a power outage in the HPS, allowing for the correction of generation and load mismatches. The DEG can be represented as a transfer function as shown below:

$$G_{DEG} = \frac{\Delta P_{DEG}}{U_2} = \frac{K_{DEG}}{1 + sT_{DEG}} \quad (6)$$

Where,  $\Delta P_{DEG}$  denotes DEG output power deviation,  $K_{DEG}$  denote gain, and  $T_{DEG}$ , denotes the time constant parameters, respectively.

#### Battery Energy Storage System (BESS)

The BESS can be used to give extra damping to power system instabilities, as well as better transient and dynamic stability. In the form of a transfer function, the BESS is described as follows:

$$G_{BESS} = \frac{\Delta P_{BESS}}{U_2} = \frac{K_{BESS}}{1 + sT_{BESS}} \quad (7)$$

Where,  $\Delta P_{BESS}$  is BESS output power deviation,  $K_{BESS}$  denote gain and  $T_{BESS}$  denote the time constant parameters.

The AVR is used to maintain the terminal voltage within prespecified limit. An AVR consists of basic fundamental components like an amplifier, exciter, generator field, sensor, and controller, as depicted in Figure 3.

#### Amplifier [3], [25]

The transfer function model for the amplifier can be described as follows.

$$G_{AMP} = \frac{\Delta V_R}{U_3} = \frac{K_{AMP}}{1 + sT_{AMP}} \quad (8)$$

#### Exciter [3], [25]

The transfer function model for the exciter can be described as follows.

$$G_{exc} = \frac{\Delta V_F}{\Delta V_R} = \frac{K_{exc}}{1 + sT_{exc}} \quad (9)$$

#### Generator field [3], [25]

The transfer function model for the generator field can be

described as follows.

$$G_{field} = \frac{\Delta V_T}{\Delta V_F} = \frac{K_{gen}}{1 + sT_{gen}} \quad (10)$$

#### Sensor [3], [25]

The transfer function model for the sensor can be described as follows.

$$G_{se} = \frac{\Delta V_S}{\Delta V_T} = \frac{K_{se}}{1 + sT_{se}} \quad (11)$$

Here  $s_i$  is the constant and is known as the coupling coefficient.  $\{i= 1, 2, 3, 4, 5\}$

#### Power and System Frequency Deviation

The various subsystems are carefully controlled to ensure the power and frequency balance of the investigated HPS. The power balancing equation can be represented as follows when using the AVR model and incorporating the small effect of voltage on real power:

$$\Delta P_e = \Delta P_{MG} + \Delta P_{TH} - \Delta P_L - P_{real} \quad (12)$$

Where,  $\Delta P_e$  denotes the deviation in system power;  $\Delta P_{MG}$  is the deviation of the output power of microgrid, whereas  $\Delta P_L$  is variation in the load perturbation,  $P_{real}$  is the power associated with the AVR. The microgrid power can be expressed as

$$\Delta P_{MG} = \Delta P_{WTG} + \Delta P_{FC} - \Delta P_{AE} + \Delta P_{DEG} \pm \Delta P_{BESS} \quad (13)$$

Where  $\Delta P_{WTG}$ ,  $\Delta P_{FC}$ ,  $\Delta P_{AE}$ ,  $\Delta P_{DEG}$  and  $\Delta P_{BESS}$  are the output power of the constitute subsystem respectively. The frequency deviation  $\Delta f$  can be defined as  $\Delta f = \Delta P_e / K_{sys}$ , where  $K_{sys}$  is the frequency related system constant. The transfer function describes system frequency and power variations mathematically:

$$G_{sys} = \frac{\Delta P_e}{K_{sys}} = \frac{1}{K_{sys}(1 + sT_{sys})} = \frac{K_p}{1 + sT_p} \quad (14)$$

### 3. CONTROL STRATEGIES AND OPTIMIZATION ALGORITHMS USED

#### A. Control Strategies

In this work, the main control approach described is a hybrid FuPID and FuPID. The application of ALO in the optimization of controller gain parameters is innovative. The hybrid controller, which combines FuPID and traditional PID controllers, can handle challenges such as robust stability and disturbance rejection [26], [27]. This study uses category one and achieve the hybrid controller structure of FuPID plus PID, as shown in Figure 4.

Controller's overall structure, as shown in Figure 4, the FuPID can be seen as group of two control structures namely Fuzzy PD and Fuzzy PI [28], [29] where  $K_1$ ,  $K_2$  are input scaling factors and  $U_f$  is the FuPID output involving  $K_{pf}$ ,  $K_{If}$  is obtained as:

$$U_f = K_{pf}u_f + K_{If} \int u_f \quad (15)$$

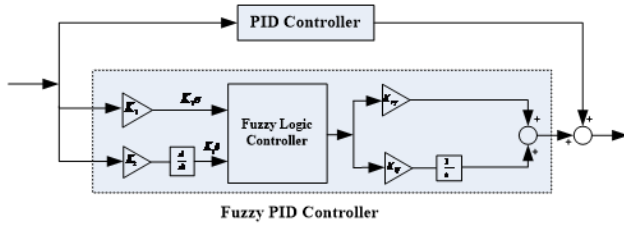


Figure 4. Hybrid Fuzzy-PID control architecture

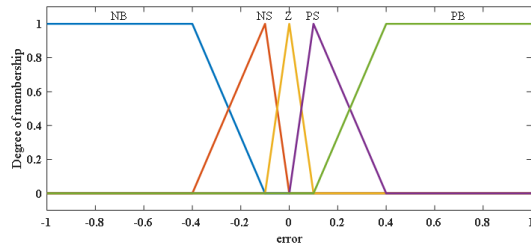


Figure 5. Fuzzy membership function

where  $u_f$  is the output of fuzzy logic controller (FLC). Now, the proposed hybrid controller's overall output can be expressed as

$$U = U_f + K_p e + K_I \int e dt + K_D e \quad (16)$$

ALO is used to optimise the controller design parameters  $K_1, K_2, K_{pf}, K_{lf}, K_p, K_I$  and  $K_D$ . In the overall HPS: Reheat Thermal Power System, Microgrid, and AVR, the controllers are connected to the control outputs:  $u_1, u_2, u_3$ , which serve as control inputs to the corresponding subsystem, as illustrated in Figure 2.

The controllers receive ACE and its rate of change as inputs. The tunable parameters are the input scaling factors:  $K_i, i = 1$  to 6, two each for the respective controller. Similarly, for the FuPID plus PID hybrid controllers tunable gain parameters are  $K_{pfj}, K_{lfj}, K_{pj}, K_{lj}, K_{Dj}$ , with  $j$  ranging from 1 to 3. The FLC membership functions and ruleset are kept fixed and are shown in Figure 5 and Table I, respectively.

For each of the three linguistic variables in this investigation, triangular membership functions were applied: ACE, its rate of change and FLC output, which are further subdivided into five linguistic values, as shown in Figure

TABLE I. Fuzzy rule base

	NB	NS	Z	PS	PB
NB	NB	NB	NS	NS	Z
NS	NB	NS	NS	Z	PS
Z	NS	NS	Z	PS	PS
PS	NS	Z	PS	PS	PB
PB	Z	PS	PS	PB	PB

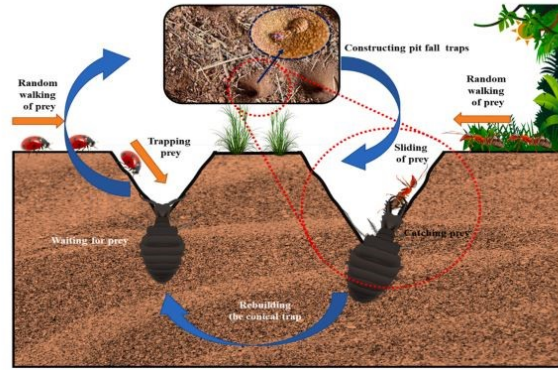


Figure 6. Ant lion hunting mechanism

5 with names NB, NS, Z, PS and PB where N, P, B, S, and Z stands for Negative, Positive, Big, Small, and Zero respectively.

B. ALO

ALO, introduced by Mirjalili [30] is a population based Metaheuristic Algorithms that attempts to replicate hunting behaviors of antlions in nature. The five essential components of hunting include ant wandering, building traps, trapping ants inside them, catching prey, and re-building traps. Three phases are used to evaluate the suggested method. They create a cone-shaped fosse in the sand by using circular jaw movements. These patient trappers will lurk at the bottom of the trap and wait for their prey to stumble onto the sharp ends. They raid to kill the prey after realising that an insect cannot flee. Figure 6 shows the hunting mechanism of the antlion.

Ants and antlions are two different types of search agents in the ALO. The finest search agents are chosen as antlions, which do not move places unless they are called upon to replace a specific ant. If an ant agent is imprisoned in a pit, it can be captured by an antlion if it wanders around the solution space at random. Using the rule in [31], ant's position can be achieved.

$$Ant_i^t = \frac{R_A^t + R_E^t}{2} \quad (17)$$

Where  $R_A^t, R_E^t$  are the stochastic process the target antlion and location of randomly walking ant nominated by the roulette wheel at  $t_{th}$  iteration with indexed  $i$ . named  $Ant_i$ , nearby the dignified antlion indexed  $E$  in the swarm of ants. In the presence of an assumed  $Antlion_j^t$ , an  $Ant_i^t$  random wandering behaviour may be represented as

$$R_j^t = \frac{(X_i - a_i) * (d_i - c_i^t)}{(b_i^t - a_i)} \quad (18)$$

Where  $R_j^t$  is the position of ant  $i$  after functioning a stochastic process near antlion  $j$  during iteration  $t$ ,  $a_i, b_i$  are the minimum and maximum step of stochastic process  $X_i^t$  in  $i_{th}$  dimension,  $X_i$  is defined by Equation 19,  $c, d$  are



the inferior and superior restraints of the stochastic process.

$$X(t) = [0, CS(2z(t_1) - 1); CS(2z(t_2) - 1); \dots; CS(2z(t_T) - 1)] \quad (19)$$

where CS stands for cumulative sum and provides a stochastic process at time t, and z(t) is a stochastic variable as shown by Equation 20

$$z(t) = \begin{cases} 1 & r > 0.5 \\ 0 & r \leq 0.5 \end{cases} \quad (20)$$

here r denotes the range of random numbers between (0, 1). The c, d are adjusted using Equation 21 and 22 to regulate the number of random travels near the presumed antlion.

$$c_i^t = \begin{cases} \frac{lb}{\alpha} + X_{Antlion_j^t} & n < 0.5 \\ \frac{-lb}{\alpha} + X_{Antlion_j^t} & otherwise \end{cases} \quad (21)$$

$$c_i^t = \begin{cases} \frac{ub}{\alpha} + X_{Antlion_j^t} & n > 0.5 \\ \frac{-ub}{\alpha} + X_{Antlion_j^t} & otherwise \end{cases} \quad (22)$$

lb, ub are the lower and upper limits for dimension i, respectively.  $\alpha$  is a component that can track the diversification/intensification ratio and is expressed as of Equation 23.

$$\alpha = 10^w \frac{t}{T_{max}} \quad (23)$$

where w,  $T_{max}$  are the iteration-specific and maximum-iteration-specific constants, respectively.

$$w = \begin{cases} 2 & t > 0.1T \\ 3 & t > 0.5T \\ 4 & t > 0.751T \\ 5 & t > 0.9T \\ 6 & t > 0.95T \end{cases} \quad (24)$$

w can be used to fine-tune the intensity accuracy. The radius of the random walk decreases as the iteration count increases, ensuring convergence of this approach. Finally, if an ant is a better solution, an ant will replace an antlion in the selection process. The ALO flowchart is shown in Figure 7.

#### 4. RESULT AND DISCUSSION

The system is investigated using the MATLAB platform in the following scenario, with qualitative and quantitative analysis of simulation results:

- Comparison of the ALO algorithm's performance
- Analysis of ALO's relative performance.
- Comparative performance of various controllers.
- Analysis of sensitivity to parametric deviations.

##### A. Comparison of the ALO algorithm's performance

The system of Figure 1 is simulated for the frequency and voltage regulation of an isolated power system subjected to a step load perturbation of 0.01 per unit to illustrate the superiority of the ALO algorithm. Programs for the aforementioned algorithms are composed in (.mfile). The suggested controller settings fall within the interval [0, 2],

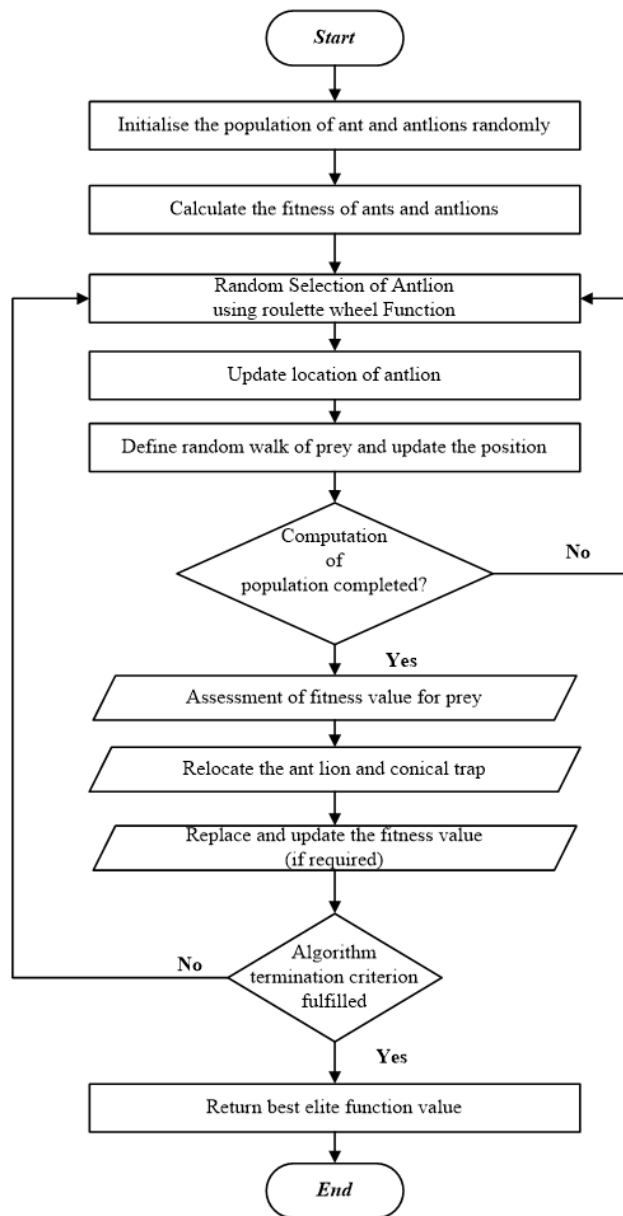


Figure 7. Flow chart of ALO optimization

and Table II compares the performance index, settling time, peak overshoot, and undershoot values to those obtained by other authors using other optimization techniques for comparable investigations. The ALO algorithm offers superior outcomes to other algorithms, as shown in Table II.

##### B. Analysis of ALO's relative performance.

In order to compare ALO's performance to that of other evolutionary optimization techniques, The performance of the system presented in Figure 2 is investigated using hybrid controllers that are optimally tuned using ALO, WOA, GWO, and SSA algorithms. WTG's average power output is assumed to be 0.5 p.u. at t = 0 s, with a 1.5% step

TABLE II. Comparative performance analysis of ALO algorithm

Optimisation technique	ALO	PSO [3]	DE [3]	GWO [3]	MVO [3]
ITAE	0.0615	0.3159	0.292	0.2714	0.271
Settling time $\Delta f$	15.865	23.413	23.02	21.843	21.838
$\Delta v$	7.0293	7.997	9.001	8.314	8.287
Peak overshoot ( $10^{-4}$ ) $\Delta f$	24.6	34.3803	34.4585	34.2913	34.2661
Peak undershoot ( $10^{-4}$ ) $\Delta v$	3.06	3.0991	2.8851	3.3871	3.3676

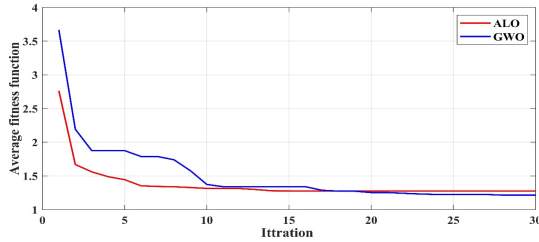


Figure 8. convergence curve

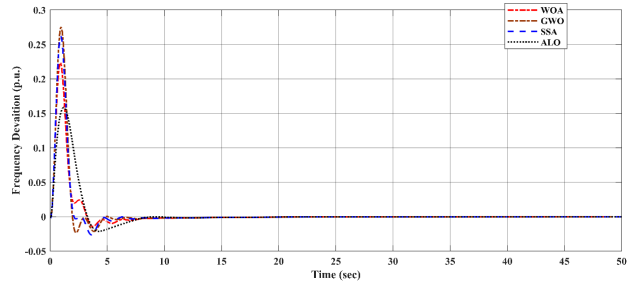


Figure 9. frequency deviation

load disturbance. All algorithms are iterated for a total of 30 times. Figure 9 and Figure 10 shows the comparative dynamic response, with Table III providing a quantitative assessment of dynamic performance with respect to ITAE value and peak overshoot, undershoot and settling time. In comparison to the other algorithms employed here, the study demonstrates that the response with ALO is less oscillatory, and the peak overshoot is also modest. This demonstrates that ALO outperforms all other algorithms used in this study. In the case of ALO, the setting time and peak overshoot value are 7.7335 and 0.1585p.u. in case of frequency deviation and peak undershoot is 0.0670 p.u. in case of voltage deviation, respectively, which is least among all other algorithm applied.

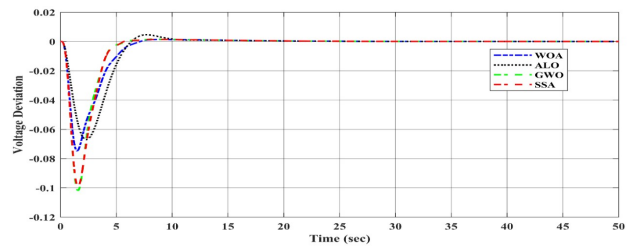


Figure 10. voltage deviation

The convergence characteristics are computed and presented in Figure 8 for the comparison of ALO with other algorithms. With respect to fitness value and rate of convergence, it is evident that ALO offers significantly greater convergence performance.

With 30 iterations and 30 population sizes, the computation costs for each algorithm are also calculated and shown in Table IV. Furthermore, as shown in table the ALO algorithm outperform to other algorithms in terms of computational cost with least cost.

C. Comparative performance of various controllers

The ALO optimised hybrid FuPID plus PID controller is used in this paper’s main premise to control the system’s frequency and voltage deviations. To assess the relative efficacy of the suggested control method, its performance is contrasted with that of conventional PI, PID, and FuPID controllers that have undergone ALO optimization. Figure 11 and Figure 12 shows the frequency and voltage regulation efficacy of all of these controllers. According to

the results, the suggested controller outperforms traditional controllers in terms of frequency deviations that are less oscillatory, have less peak overshoot and undershoot, and die down more quickly. The parameter values in Table V show similar relative performance. In the case of a hybrid FuPID + PID controller, the ITAE value and settling time are 0.1161 and 7.2461 sec respectively, which is the lowest of all controllers. In addition, the peak overshoot value is 0.0241 p.u. and undershoot is 0.0670 p.u., which is again the lowermost with suggested controller.

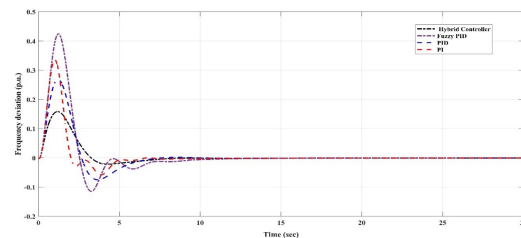


Figure 11. controller comparison with respect to frequency deviation



TABLE III. Qualitative performance parameter with different algorithm

Parameters	ALO	GWO	SSA	WOA
ITAE	<b>1.0904</b>	1.2148	1.2121	1.2749
Frequency deviation ( $\Delta f$ )	Settling time (sec)	<b>3.7335</b>	4.5044	5.6722
	Overshoot (p.u.)	<b>0.1585</b>	0.27505	0.26189
Voltage Deviation ( $\Delta v$ )	Settling time (sec)	<b>10.4715</b>	5.1315	5.201
	Undershoot (p.u.)	<b>0.067</b>	0.1019	0.0991
<b>Fuzzy-PID Controller parameters</b>				
K1	<b>1</b>	0.6742	0.9612	1
K2	<b>1</b>	0.4396	0.691	1
Kpf1	<b>0.9965</b>	0.3476	0.3717	0.41539
Kif1	<b>1</b>	0.8687	0.919	1
K3	<b>0.9856</b>	0.0132	0.5578	0.61772
K4	<b>0.5677</b>	0.0132	0.1558	1
Kpf2	<b>1</b>	0.2636	0.3427	1
Kif2	<b>0.9723</b>	0.4291	0.862	0
<b>PID Controller parameters</b>				
Kp1	<b>0.9963</b>	1	0.9642	1
Ki1	<b>1</b>	1	0.9845	1
Kd1	<b>0.4454</b>	0.0404	7.02E-05	0
Kp2	<b>0.9356</b>	0.0978	0.9881	0
Ki2	<b>0.6122</b>	0.5038	0.9871	0
Kd2	<b>0.2937</b>	0.8312	0.115	0
<b>AVR Controller (Fuzzy PID plus PID) parameters</b>				
K5	<b>1.9995</b>	2	2	2
K6	<b>2</b>	1.8658	0.5048	2
Kpf3	<b>1.9903</b>	0.847	1.9478	2
Kif3	<b>2</b>	2	1.9997	2
Kp3	<b>2</b>	1.7235	1.6529	2
Ki3	<b>2</b>	2	2	2
Kd3	<b>1.9692</b>	0.1833	0.1844	0

TABLE IV. The computational cost of all algorithms

S. No	Optimization	Run Time (sec)
1	ALO	083783.376079
2	GWO	097590.554935
3	SSA	103768.847328
4	WOA	099918.340996

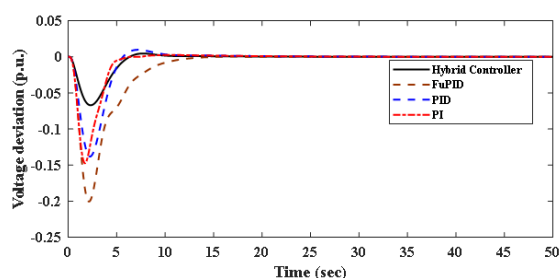


Figure 12. controller comparison with respect to voltage deviation

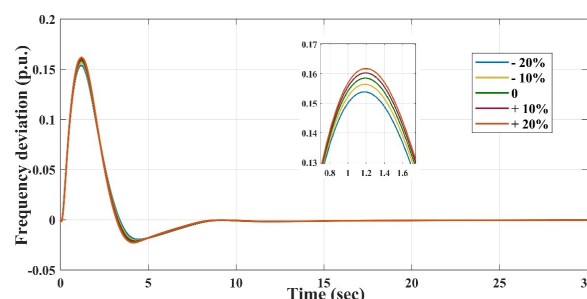


Figure 13. sensitive analysis of HPS

#### D. Analysis of sensitivity to parametric deviations

The suggested ALO tuning optimised hybrid controller is evaluated regarding sensitivity analysis considering system parametric fluctuation. Figure 13 shows the frequency deviation in HPS under the influence of variation in systems parameter by  $\pm 10\%$  and  $\pm 20\%$ , while maintaining the optimal value of controller gains, obtained using ALO. Figure 13 shows that the suggested hybrid controller with ALO tuning is resilient and steady over parametric fluctuations over a broad range without degrading the controller's



TABLE V. Parameter with different controllers

Controllers		PI	PID	FuPID	Hybrid Controller
ITAE		2.3086	3.0339	4.567	<b>1.0904</b>
Frequency deviation ( $\Delta f$ )	Settling time (sec)	6.0656	6.742	9.1609	<b>3.7335</b>
	Overshoot (p.u.)	0.3355	0.2691	0.4229	<b>0.1585</b>
Voltage deviation ( $\Delta v$ )	Settling time (sec)	5.485	10.4766	11.3956	<b>10.4715</b>
	Undershoot (p.u.)	0.1473	0.1381	0.2005	<b>0.067</b>
<b>Controller parameters</b>					
K1		-	-	0.9983	<b>1</b>
K2		-	-	0.4061	<b>1</b>
Kpf1		-	-	0.9774	<b>0.9965</b>
Kif1		-	-	1	<b>1</b>
K3		-	-	0.4992	<b>0.9856</b>
K4		-	-	0.8933	<b>0.5677</b>
Kpf2		-	-	0.8957	<b>1</b>
Kif2		-	-	0.9974	<b>0.9723</b>
Kp1		1	0.7389	-	<b>0.9963</b>
Ki1		1	1	-	<b>1</b>
Kd1		-	0.3779	-	<b>0.4454</b>
Kp2		0.8637	0.6917	-	<b>1.0904</b>
Ki2		0.8462	0.6992	-	<b>3.7335</b>
Kd2		-	0.9876	-	<b>0.1585</b>
K5		-	-	2	<b>1.9995</b>
K6		-	-	1.9872	<b>2</b>
Kpf3		-	-	1.9192	<b>1.9903</b>
Kv		-	-	2	<b>2</b>
Kp3		2	2	-	<b>2</b>
Ki3		2	1.9504	-	<b>2</b>
Kd3		-	1.4017	-	<b>1.9692</b>

optimum gain.

## 5. CONCLUSIONS AND FUTURE WORK

In this study, HPS encircling a conventional reheated thermal system, and a Microgrid, which consist a variety of sources such as WTG, DEG, BESS, FC, and AE, hybrid FuPID plus PID controller is suggested for the voltage and frequency control. With ALO, each controller's parameter is optimised. Both the ALO and the proposed controller were found to be superior in terms of performance in a comparison of ALO with other evolutionary optimization algorithms: GWO, SSA, and WOA as well as the proposed controller with PI, PID and Fuzzy PID. Based on simulations results, it was found that ALO tuned proposed controller effectively improves the overshoot by 57.62%, 60.52%, 70.95%, undershoot by 65.75%, 67.60%, 89.57%, settling time by 82.88%, 65.82%, 51.06% respectively when proposed controller is tuned with GWO, SSA and WOA. Furthermore, the ALO tuned proposed controller shows improvement in performance index (ITAE) and settling time by 47.23% and 61.55%, 35.94% and 55.37%, 23.87% and 40.75% respectively when compared with PI, PID and FuPID. The research is presented as a series of case studies. Under various operating conditions of HPS, proposed control technique has proven to be effective and resilient. As per sensitivity analysis, The ALO tuned hybrid FuPID +

PID controller is highly effective in controlling voltage and frequency deviations over a wide variety of parametric variations. The research can be furthered by contrasting efficacy of the suggested controller and optimization techniques on the hybrid microgrid model with other novel controllers and very recent algorithms in subsequent work. In our future work, we may also take into account using some real-time data while doing case studies with real-time systems like OPAL-RT.

## APPENDIX

### System parameters

$f = 50\text{Hz}$ ;  $K_g = 1.0$ ;  $T_g = 0.08\text{s}$ ;  $R = 2.4$ ;  $K_p = 120\text{Hz/p.u.MW}$ ;  $T_P = 20\text{s}$ ;  $K_{TWG} = 1.0$ ;  $T_{TWG} = 1.5\text{s}$ ;  $K_{AE} = 1.0$ ;  $T_{AE} = 0.08\text{s}$ ;  $K_{FC} = 0.01$ ;  $T_{FC} = 4\text{s}$ ;  $K_{DEG} = 0.03\text{s}$ ;  $T_{FEG} = 2\text{s}$ ;  $K_{BESS} = -0.003$ ;  $T_{BESS} = 0.1\text{s}$ ;  $K_{AMP} = 10$ ;  $T_{AMP} = 0.1\text{s}$ ;  $K_{exc} = 1$ ;  $T_{exc} = 0.4\text{s}$ ;  $K_{gen} = 0.04$ ;  $T_{gen} = 0.7\text{s}$ ;  $K_{se} = 1$ ;  $T_{se} = 0.05\text{s}$ ;  $s_1 = 0.5$ ;  $s_2 = 1.4$ ;  $s_3 = 1$ ;  $s_4 = -0.5$ ;  $s_5 = 0.145$ ;

## REFERENCES

- [1] O. Olabode, T. Ajewole, I. Okakwu, A. Alayande, and D. Akinyele, "Hybrid power systems for off-grid locations: A comprehensive review of design technologies, applications and future trends," *Scientific African*, vol. 13, p. e00884, 2021.





- [2] J. P. Lopes, N. Hatziaargyriou, J. Mutale, P. Djapic, and N. Jenkins, "Integrating distributed generation into electric power systems: A review of drivers, challenges and opportunities," *Electric power systems research*, vol. 77, no. 9, pp. 1189–1203, 2007.
- [3] D. K. Lal and A. K. Barisal, "Combined load frequency and terminal voltage control of power systems using moth flame optimization algorithm," *Journal of Electrical Systems and Information Technology*, vol. 6, no. 1, pp. 1–24, 2019.
- [4] Y. Arya, "Improvement in automatic generation control of two-area electric power systems via a new fuzzy aided optimal pidn-foi controller," *ISA transactions*, vol. 80, pp. 475–490, 2018.
- [5] N. Hakimuddin, A. Khosla, and J. K. Garg, "Centralized and decentralized agc schemes in 2-area interconnected power system considering multi source power plants in each area," *Journal of King Saud University-Engineering Sciences*, vol. 32, no. 2, pp. 123–132, 2020.
- [6] A. Kumar and S. Suhag, "Gwo algorithm based fuzzy-pid controller with derivative filter for load frequency control of multi-source hydrothermal power system," in *Proceedings of the 2017 The 5th International Conference on Control, Mechatronics and Automation*, 2017, pp. 50–55.
- [7] M. Sharma, S. Prakash, and S. Saxena, "Robust load frequency control using fractional-order tid-pd approach via salp swarm algorithm," *IETE Journal of Research*, pp. 1–17, 2021.
- [8] L. Dritsas, E. Kontouras, E. Vlahakis, I. Kitsios, G. Halikias, and A. Tzes, "Modelling issues and aggressive robust load frequency control of interconnected electric power systems," *International Journal of Control*, vol. 95, no. 3, pp. 753–767, 2022.
- [9] D. Mohanty and S. Panda, "Frequency control of hybrid power system by sine function adapted improved whale optimisation technique," *International Journal of Ambient Energy*, vol. 43, no. 1, pp. 3518–3535, 2022.
- [10] S. Mostafa Bozorgi and S. Yazdani, "Iwoa: An improved whale optimization algorithm for optimization problems," *Journal of Computational Design and Engineering*, vol. 6, no. 3, pp. 243–259, 2019.
- [11] Y. Arya, "A novel cffopi-fopid controller for agc performance enhancement of single and multi-area electric power systems," *ISA transactions*, vol. 100, pp. 126–135, 2020.
- [12] D. Abdelmoumene, A. Salem, and M. Lakhdar, "Load frequency control problem in interconnected power systems using robust fractional pikd controller," *Ain Shams Eng J*, vol. 9, pp. 77–88, 2018.
- [13] Q. Zhong, J. Yang, K. Shi, S. Zhong, Z. Li, and M. A. Sotelo, "Event-triggered  $h_{\infty}$  load frequency control for multi-area nonlinear power systems based on non-fragile proportional integral control strategy," *IEEE Transactions on Intelligent Transportation Systems*, 2021.
- [14] X. Liang, X. Li, R. Lu, X. Lin, and X. Shen, "Udp: Usage-based dynamic pricing with privacy preservation for smart grid," *IEEE Transactions on smart grid*, vol. 4, no. 1, pp. 141–150, 2013.
- [15] A. Dutta and S. Prakash, "Utilizing electric vehicles and renewable energy sources for load frequency control in deregulated power system using emotional controller," *IETE Journal of research*, vol. 68, no. 2, pp. 1500–1511, 2022.
- [16] A. Ghasemi-Marzbali, "Multi-area multi-source automatic generation control in deregulated power system," *Energy*, vol. 201, p. 117667, 2020.
- [17] S. J. Yeboah *et al.*, "Gravitational search algorithm based automatic load frequency control for multi-area interconnected power system," *Turkish Journal of Computer and Mathematics Education (TURCOMAT)*, vol. 12, no. 3, pp. 4548–4568, 2021.
- [18] A. Kumar *et al.*, "Hybrid bacterial foraging enhanced pso algorithm for load frequency control of hydro-thermal multi-area power system and comparative analysis," *International Journal of Computing and Digital Systems*, vol. 9, no. 1, 2020.
- [19] J. R. Giri, N. Parvez, D. K. Mishra, A. Das, and S. Jena, "Robust automatic generation control in two area thermal-hydro-nuclear plant with 2dofpid controller," in *2018 Technologies for Smart-City Energy Security and Power (ICSESP)*. IEEE, 2018, pp. 1–5.
- [20] M. K. Debnath, J. R. Padhi, P. Satapathy, and R. K. Mallick, "Application of jaya algorithm to tune fuzzy-pidf controller for automatic generation control," in *2017 3rd International Conference on Computational Intelligence and Networks (CINE)*. IEEE, 2017, pp. 94–98.
- [21] A. Panwar, G. Sharma, and R. C. Bansal, "Optimal agc design for a hybrid power system using hybrid bacteria foraging optimization algorithm," *Electric Power Components and Systems*, vol. 47, no. 11-12, pp. 955–965, 2019.
- [22] A. Kumar and S. Suhag, "Whale optimization algorithm optimized fuzzy-pid plus pid hybrid controller for frequency regulation in hybrid power system," *Journal of The Institution of Engineers (India): Series B*, vol. 103, no. 2, pp. 633–648, 2022.
- [23] V. Mukherjee and S. Ghoshal, "Comparison of intelligent fuzzy based agc coordinated pid controlled and pss controlled avr system," *International Journal of Electrical Power & Energy Systems*, vol. 29, no. 9, pp. 679–689, 2007.
- [24] P. K. Ray, S. R. Mohanty, and N. Kishor, "Proportional–integral controller based small-signal analysis of hybrid distributed generation systems," *Energy Conversion and Management*, vol. 52, no. 4, pp. 1943–1954, 2011.
- [25] S. Gupta, *Power System Operation Control & Restructuring*. IK International Publishing House, 2015.
- [26] Q. Zhi, "Pid type fuzzy controller and parameters adaptive method," *Fuzzy Sets and Systems*, vol. 90, no. 1, pp. 103–103, 1997.
- [27] W. Li, "Design of a hybrid fuzzy logic proportional plus conventional integral-derivative controller," *IEEE transactions on fuzzy systems*, vol. 6, no. 4, pp. 449–463, 1998.
- [28] A. Rubaai, M. J. Castro-Sitiriche, and A. R. Ofoli, "Dsp-based laboratory implementation of hybrid fuzzy-pid controller using genetic optimization for high-performance motor drives," *IEEE transactions on industry applications*, vol. 44, no. 6, pp. 1977–1986, 2008.
- [29] R. Storn and V. Kenneth, "Price, k.: Differential evolution—a simple and efficient adaptive scheme for global optimization over continuous spaces," *International Computer Science Institute, Report no. TR-95-012, Berkeley*, 1995.
- [30] M. Seyedali, "The ant lion optimizer," *Advances in engineering software*, vol. 83, pp. 80–98, 2015.



- [31] S. Mirjalili, J. S. Dong, and A. Lewis, "Nature-inspired optimizers," *Cham, Switzerland: Springer*, pp. 69–85, 2020.



**Sanni Kumar** is pursuing his Phd in the area of Control Issues in Hybrid Power system from from the National Institute of Technology Kurukshetra, Haryana, India. His research interest include bio-inspired computing methods, evolutionary optimization algorithms etc. and their application in Hybrid Power system.



**Amit Kumar** received his PhD degree in the area of load frequency control and modern heuristic optimization techniques in hybrid power system from the National Institute of Technology Kurukshetra, Haryana, India, in 2018 where he is currently serving as Assistant Professor. His research interests include bio-inspired computing methods, evolutionary optimization algorithms etc. and their applications in power system.